12. K. T. Jones, M. Matsud, J. Parrigton, M. Katan, K. Swann, *Biochem. J.* **346**, 743 (2000).
13. P. M. Wasserman, *Cell* **96**, 175 (1999).
14. M. N. Llanos, *Mol. Reprod. Dev.* **51**, 84 (1998).
15. H. M. Florman, *Dev. Biol.* **165**, 152 (1994).
16. H. Shirakawa, S. Miyazaki, *Dev. Biol.* **208**, 70 (1999).
17. C. M. B. O'Toole, C. Arnoult, A. Darszon, R. A. Sternhardt, H. M. Florman, *Mol. Biol. Cell* **11**, 1571 (2000).
18. J. P. Nolan, R. H. Hammerstedt, *FASEB J.* **11**, 670 (1997).
19. P. E. Visconti *et al.*, *J. Biol. Chem.* **274**, 3235 (1999).
20. E. Kaznacheyeva *et al.*, *J. Biol. Chem.* **275**, 4561 (2000).
21. Phage clones containing the first coding exon of PLCδ4 were isolated from a FIXII mouse genomic library (strain 129SV/J). The linearized targeting vector was electroporated into 129SV/J ES cells. Chimeric males were bred to C57BL/6J females and DNA samples from the tail of agouti offspring were analyzed by Southern blotting.
22. For immunohistochemistry, adult testes from PLCδ4$^{+/+}$ or PLCδ4$^{-/-}$ mice were fixed in 4.0% formaldehyde, embedded in paraffin, and thin sections were treated with a procedure described in the Technical Bulletin of the TSA immunodetection kit (NEN). For Western blot analysis, 30 μg of homogenates of testis, epididymis, or sperm were subjected to SDS–polyacrylamide gel electrophoresis and electrically transferred onto a polyvinylidene difluoride membrane. The membranes were then incubated with antibodies against PLC isozymes (Santa Cruz Biotechnology). For immunostaining, sperm were fixed with 3.7% formaldehyde for 1 hour, permeabilized with phosphate-buffered saline (PBS) containing 0.2% Triton X-100 for 5 min, and then incubated with antibody against PLCδ4 for 1 hour.
23. Fresh cauda epididymal sperm were capacitated for 1 hour in modified Krebs-Ringer (TYH) medium. A drop of sperm suspension (0.1 to 0.2 × 10^6 sperm per milliliter) was added to the medium containing eggs from wild-type mice. Embryo development was followed by microscopic observation. For measuring calcium oscillation, cumulus cells were removed by brief exposure to hyaluronidase, and the zona pellucida was removed by exposure to acid tyrode's solution (pH 2.5). Eggs were loaded at 37°C for 30 min with 3 μM calcium green I-AM (Molecular Probes). Fertilization-induced changes in intracellular calcium concentrations were measured by using confocal microscopy at 37°C.
24. Sperm were collected into PBS and frozen in liquid nitrogen. After thawing, a single sperm head was injected per egg. ICSI was performed on eggs kept in 50-μl drops of tyrode lactate–Hepes + 5% fetal bovine serum at 18° to 19°C as described before (*11*). Following ICSI, eggs were subjected to calcium monitoring.
25. C. R. Ward, B. T. Storey, G. S. Kopf, *J. Biol. Chem.* **267**, 14061 (1992).
26. We would like to thank Y. Morishita, Y. Fukamizu, and Y. Kabayama (The University of Tokyo), for advice with immunohistochemistry, in vitro fertilization, and for assistance with antibody production and immunostaining, respectively. We also thank H. Wu, and C. L. He (University of Massachusetts) for help with calcium monitoring.

16 January 2001; accepted 3 April 2001

Control of Glutamate Clearance and Synaptic Efficacy by Glial Coverage of Neurons

Stéphane H. R. Oliet,* Richard Piet, Dominique A. Poulain

Analysis of excitatory synaptic transmission in the rat hypothalamic supraoptic nucleus revealed that glutamate clearance and, as a consequence, glutamate concentration and diffusion in the extracellular space, is associated with the degree of astrocytic coverage of its neurons. Reduction in glutamate clearance, whether induced pharmacologically or associated with a relative decrease of glial coverage in the vicinity of synapses, affected transmitter release through modulation of presynaptic metabotropic glutamate receptors. Astrocytic wrapping of neurons, therefore, contributes to the regulation of synaptic efficacy in the central nervous system.

Astrocytes contribute to the regulation of synaptic transmission by controlling glutamate diffusion and concentration in the extracellular space (*1–3*). Changes in the glial coverage of neurons in the vicinity of synapses may thus alter glutamate clearance and synaptic transmission (*4*). To examine the effect of changes in glial coverage on synaptic transmission, we recorded from the magnocellular nuclei of the hypothalamus, which undergo a well-documented anatomical neuroglial plasticity in response to intense stimulation, like lactation (*5, 6*). This results in a decreased coverage of neurons by astrocytic processes and a relative absence of these processes in the vicinity of the synapses. The changes are reversed with cessation of stimulation in postlactating animals.

To investigate such neuroglial interactions, we first examined the functional consequences of a glutamate clearance deficiency on excitatory synaptic transmission. We inhibited glutamate transporters in the rat supraoptic nucleus (SON) with either dihydrokainate (DHK)—a specific inhibitor of GLT-1 (*7, 8*), a glutamate transporter exclusively expressed in astrocytes (*9–11*)—or L-trans-pyrrolidine-2,4-dicarboxylic acid (PDC), a broad-spectrum glutamate transporter blocker (*8*). In virgin rats, where glial coverage is extensive (*5, 6*), whole-cell voltage-clamp recordings (*12*) of SON neurons revealed that evoked excitatory postsynaptic currents (EPSCs) were inhibited reversibly (Fig. 1, A and B) by 100 μM DHK (46.6 ± 8.0% of control values, $n = 9$) and 300 μM PDC (51.2 ± 6.8%, $n = 12$). That PDC and DHK depressed evoked EPSCs to the same extent suggests that, for the most part, their effect was mediated by inhibition of GLT-1 transporters, which are present only on astrocytes in this and other brain areas (*11*). The depression in EPSC amplitude induced by glutamate transporter antagonists was associated with an increase in the paired-pulse facilitation (PPF) ratio (*13*), from 1.2 ± 0.1 to 1.6 ± 0.2 (40-ms interval; $P < 0.05$, $n = 6$). Analysis of miniature EPSCs (mEPSCs) (Fig. 1, C to E) revealed that PDC decreased the frequency (−34.0 ± 6.1%; $P < 0.05$, $n = 6$), but not the size (−1.6 ± 4.3%; $P > 0.05$), of these events (Fig. 1F). This indicates that the decrease in excitatory synaptic transmission associated with blockade of glutamate transporters had a presynaptic origin.

These effects could result from a local build-up of glutamate that would lead to activation of presynaptic glutamate receptors controlling neurotransmitter release (*14, 15*). Group III metabotropic glutamate receptors (mGluRs) are known to induce a presynaptic inhibition in the SON (*16*). We thus investigated the action of PDC in the presence of L-2-amino-4-phosphonobutyric acid (L-AP4) and 2-amino-2-methyl-4-phosphonobutanoic acid (MAP4), an agonist and an antagonist of group III mGluRs, respectively (Fig. 2, A and C). Whereas L-AP4 (200 μM) impaired evoked EPSCs (19.6 ± 2.8%; $P < 0.05$, $n = 5$), subsequent addition of PDC had no further effect on EPSC amplitude (22.8 ± 3.0%; $P > 0.05$, $n = 5$). In contrast, 250 μM MAP4 increased EPSC amplitude (130.0 ± 10.0%; $P < 0.05$, $n = 9$), confirming the existence of a tonic activation of these receptors (*16*). MAP4 prevented the effects of PDC (131.2 ± 14.5%; $P > 0.05$, $n = 5$). These findings indicate that blockade of glutamate transporters in the SON modifies the concentration and/or diffusion of glutamate in the extracellular space, leading to activation of presynaptic group III mGluRs and inhibition of glutamate release.

To investigate whether similar changes in excitatory synaptic transmission occurred under physiological conditions that modify glial coverage of SON neurons, we examined hypothalamic slices obtained from lactating and postlactating animals. Glutamate transporter blockade was less effective in reducing

INSERM U.378, Université Victor Segalen–Bordeaux 2, 33077 Bordeaux, France.

*To whom correspondence should be addressed: E-mail: stephane.oliet@bordeaux.inserm.fr

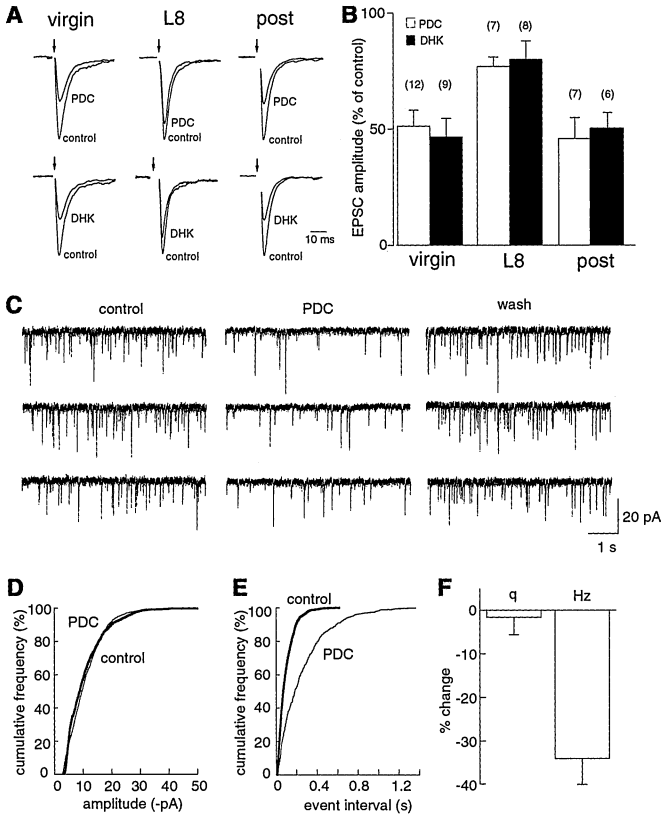

Fig. 1. Glutamate transporter blockade induces presynaptic inhibition of EPSCs. (**A**) Sample traces of evoked EPSCs obtained in SON neurons in the presence and absence of PDC (upper panel) or DHK (lower panel). Traces are averages of 10 consecutive responses obtained from virgin, lactating (L8), and postlactating (post) rats. For illustrative purposes, EPSCs are scaled to responses obtained in virgin rats under control conditions. Stimulus artifacts are removed (arrow). (**B**) Summary histogram of the inhibitory actions of PDC and DHK on evoked EPSCs in the three groups of animals. In each group, the reduction obtained with PDC was not statistically different from that obtained with DHK ($P > 0.05$); the number of cells is indicated in parentheses. (**C**) Example of a cell showing PDC-induced reduction in mEPSC activity. The corresponding cumulative amplitude distributions (**D**) obtained in the presence and absence of PDC were not statistically different ($P > 0.05$), whereas the cumulative event interval distribution (**E**) was significantly shifted to the right with PDC ($P > 0.05$), which corresponds to a reduction in mEPSC frequency. (**F**) Summary of the effects of PDC on mEPSC size (q) and frequency (Hz) observed in six different cells.

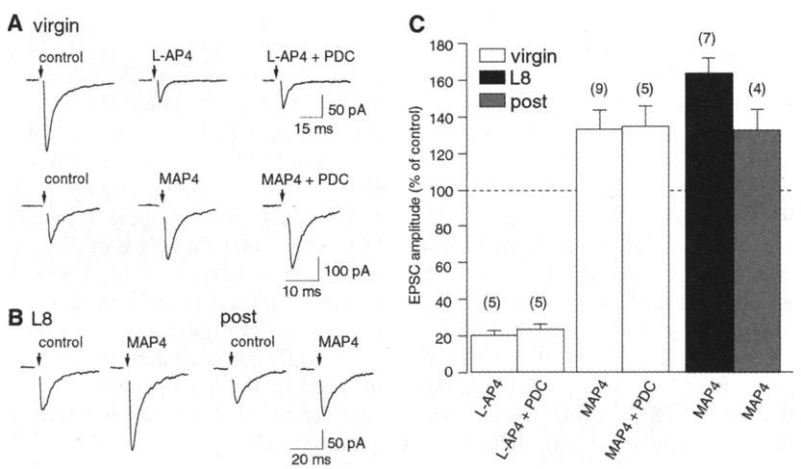

Fig. 2. Glutamate transporter blockade activates presynaptic group III mGluRs. (**A**) Sample traces of evoked EPSCs obtained in virgin rats in the absence and presence of group III mGluR agonist (L-AP4, upper panel) and antagonist (MAP4, lower panel). Subsequent application of PDC had no significant effect on EPSCs amplitude under both conditions. (**B**) Sample traces of evoked EPSCs obtained in the presence and absence of MAP4 in lactating (L8) and postlactating (post) rats. (**C**) Summary graph illustrating the changes in EPSC amplitude measured in virgin, lactating, and postlactating animals under different conditions; the number of cells is indicated in parentheses.

evoked EPSCs in lactating rats (Fig. 1, A and B). Application of either DHK or PDC depressed EPSCs to 78.2 ± 10.3% ($n = 8$) and 75.0 ± 5.1% ($n = 7$) of control values, respectively. EPSC inhibition elicited by glutamate transporter blockade in postlactating animals was similar to that recorded in virgin rats (50.4 ± 7.4% in DHK, $n = 8$, and 46.6 ± 8.0% in PDC, $n = 7$) (Fig. 1, A and B). It appears, therefore, that the inhibitory action of glutamate transporter blockers on EPSCs is correlated with the degree of glial coverage of neurons. To determine whether reduction in astrocytic coverage affects presynaptic group III mGluRs, we compared the effect of MAP4 on EPSC amplitude in the three groups of animals. MAP4 induced a larger increase ($P < 0.05$) of evoked EPSC amplitude (163.3 ± 12.1%, $n = 7$) (Fig. 2, B and C) than observed in virgin or postlactating (129.1 ± 11.3%, $n = 4$) rats. This is in agreement with an increase in tonic activation of mGluRs by ambient glutamate in lactating rats.

We next examined whether glutamate clearance deficiency also affects glutamate concentration and/or time course in the synaptic cleft (*17*, *18*), using γ-D-glutamylglycine (γ-DGG), a low-affinity, competitive AMPA receptor antagonist whose effect is sensitive to the concentration and/or time course of glutamate in the synaptic cleft (*19*). γ-DGG (0.5 mM) significantly ($P < 0.05$) reduced mEPSC amplitude, to 49.1 ± 3.3% ($n = 8$, virgin rats) and to 50.5 ± 2.9% ($n = 5$, postlactating rats) of control values (Fig. 3). Addition of PDC in the presence of γ-DGG restored mEPSC amplitude to 67.0 ± 5.1% and to 63.5 ± 6.2% in virgin ($P < 0.05$) and postlactating rats ($P < 0.05$), respectively. In contrast, inhibition of mEPSCs (46.5 ± 5.8%, $n = 6$, virgin rats; 49.4 ± 6.1%, $n = 5$, postlactating rats) by CNQX (6-cyano-7-nitroquinoxaline-2,3-dione, 500 nM) was not affected by PDC (44.0 ± 4.2% and 50.8 ± 3.9%, respectively; $P > 0.05$), as expected from a high-affinity, slowly dissociating, competitive AMPA receptor antagonist (*19*). In slices from lactating rats, the γ-DGG–induced inhibition was smaller than in virgin and postlactating rats (67 ± 4%; $P < 0.05$, $n = 11$) and was unaffected by PDC (64 ± 4%; $P > 0.05$). Moreover, in lactating rats, the reduction of mEPSC amplitude by CNQX was similar to that measured in virgin and postlactating rats (45 ± 4%, $n = 6$) and was unaffected by PDC (46 ± 4%; $P > 0.05$). These data strongly suggest that the concentration and/or time course of glutamate in the synaptic cleft is indeed greater in lactating than in virgin and postlactating rats.

Taken together, our findings indicate that reduced astrocytic coverage of SON neurons in lactating rats leads to a glutamate clearance deficiency, resulting in en-

hanced glutamate concentration in the extracellular space, increased activation of presynaptic mGluRs, and thus, presumably, to a lower probability (Pr) of glutamate release. In agreement with this hypothesis, the PPF ratio measured for short intervals (40 to 80 ms) was greater ($P < 0.05$) in lactating rats (Fig. 4A). Furthermore, in lactating animals, MAP4 restored the PPF ratio to values measured in virgin and postlactating animals, whereas in the latter, PDC increased PPF to values similar to those measured in lactating rats (Fig. 4B). Although we cannot exclude alterations in composition and/or number of postsynaptic receptors in lactating animals, as has been shown for GABA-A receptors (*20*), such modifications cannot account for the changes in Pr revealed by PPF measurements. These findings demonstrate, therefore, that astroglial wrapping of SON neurons, by controlling glutamate clearance by way of the DHK-sensitive GLT-1 transporter, plays a significant role in regulating the efficacy of glutamatergic neurotransmission.

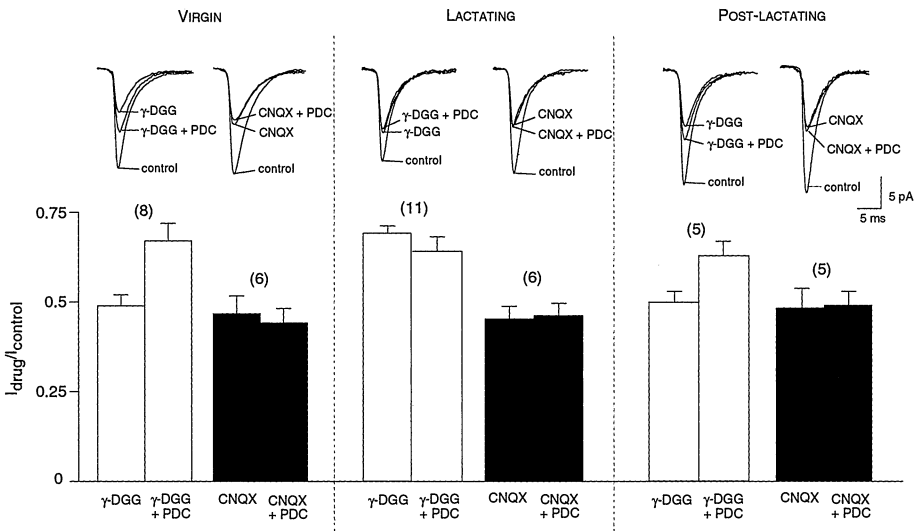

Fig. 3. Glial coverage of SON neurons affects the relative glutamate concentration and/or time course in the synaptic cleft. Summary graph illustrating the inhibition of mEPSCs observed under different conditions in virgin, lactating, and postlactating animals. Data are expressed as the ratio ($I_{drug}/I_{control}$) of the average mEPSC amplitude measured in the presence of a given drug (I_{drug}) and the average mEPSC amplitude obtained under control conditions ($I_{control}$). Averages of mEPSCs obtained under the different conditions are shown above the histograms (the number of cells is indicated in parentheses).

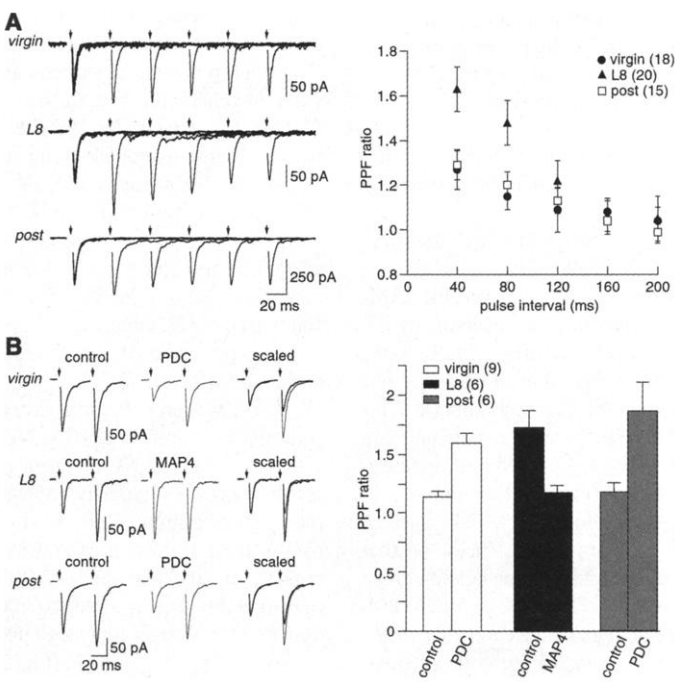

Fig. 4. Differences in transmitter release associated with neuroglial remodeling. (**A**) Superimposed traces obtained from virgin, lactating, and postlactating animals where paired-pulse stimulation was given at various intervals (left); the summary graph (right) illustrates the paired-pulse ratio measured in the three groups of animals. (**B**) Responses elicited 40 ms apart in the presence and absence of PDC for virgin and postlactating rats, and in the presence and absence of MAP4 for lactating animals (left). The corresponding summary graph illustrates the PPF ratio (right); the number of cells is indicated in parentheses.

Presynaptic inhibition can be overcome, to some extent, by frequency-dependent facilitation of transmitter release. Thus, it could serve as a high-pass filter reducing nonspecific background activity and increasing signal-to-noise ratio for information transmitted through high-frequency bursts of afferent synaptic potentials. Such a process would be favored by a relatively low degree of glial coverage of neurons, allowing an enhanced level of activation of presynaptic glutamate receptors. In hypothalamic magnocellular nuclei in particular, this mechanism may contribute to the synaptically driven high-frequency bursts of action potentials (40 to 80 Hz) characterizing oxytocinergic neurons during milk ejection (*21*, *22*). In addition to modulating transmitter release (*14*, *15*), variations in glutamate concentration associated with neuroglial remodeling could also affect the amplitude and/or time course of EPSCs (*17*, *18*), glutamate spillover (*14*, *23*), and glutamate receptors on glial cells (*24*). Such modulations of neuronal and glial activity are probably relevant in other brain functions in which such plasticity has been implicated, including learning, control of development, and estrous cycle (*25*–*27*).

References and Notes

1. J. D. Rothstein *et al.*, *Neuron* **16**, 675 (1996).
2. D. E. Bergles, C. E. Jahr, *J. Neurosci.* **18**, 7709 (1998).
3. K. Tanaka *et al.*, *Science* **276**, 1699 (1999).
4. M. El Majdoubi, D. A. Poulain, D.T. Theodosis, *Biochem. Cell Biol.* **78**, 317 (2000).
5. D. T. Theodosis, D. A. Poulain, *Neuroscience* **57**, 501 (1993).
6. G. I. Hatton, *Annu. Rev. Neurosci.*, **20**, 375 (1997).
7. G. A. R. Johnston, S. M. E. Kennedy, B. Twitchin, *J. Neurochem.* **32**, 121 (1979).
8. J. L. Arriza *et al.*, *J. Neurosci.* **14**, 5559 (1994).
9. R. Torp *et al.*, *Eur. J. Neurosci.* **6**, 936 (1994).
10. F. A. Chaudry *et al.*, *Neuron* **15**, 711 (1995).
11. K. P. Lehre, L. M Levy, O. P. Ottersen, J. Storm-Mathisen, N. C. Danbolt, *J. Neurosci.* **15**, 1835 (1995).
12. Hypothalamic coronal slices (300 μm), including the supraoptic nuclei, were obtained as described (*28*) from virgin (1- to 2-month-old), lactating (8th day of lactation), and postlactating (at least 6 weeks after weaning) Wistar rats. After dissection, slices were maintained at 30° to 34°C for at least 1 hour in a submerged chamber containing artificial cerebrospinal fluid (ACSF) equilibrated with 95% O_2 and 5% CO_2, and then transferred to a superfusing chamber. The ACSF contained (in mM) 123 NaCl, 2.5 KCl, 1 Na_2HPO_4, 26.2 $NaHCO_3$, 1.3 $MgCl_2$, 2.5 $CaCl_2$, and 10 glucose (pH 7.4; 295 mosmol kg^{-1}). Whole-cell

recording electrodes were filled with a solution containing (in mM) 120 K-gluconate, 20 KCl, 10 Hepes, 1 EGTA, 1.3 $MgCl_2$, 0.1 $CaCl_2$, 2 Mg-ATP, 0.3 GTP, and 0.1 leupeptin. All recordings were obtained in the presence of 10 μM bicuculline. Miniature EPSCs obtained in the presence of tetrodotoxin (0.5 μM) were stored on videotape and analyzed off-line. Data were compared statistically with the nonparametric Kolmogorov-Smirnov test or the paired Student's *t* test. Significance was assessed at $P < 0.05$. All data are reported as the mean ± SEM.

13. PPF is expressed as the amplitude ratio (S2/S1) of the second synaptic response (S2) over the first synaptic response (S1).
14. M. Scanziani, P. A. Salin, K. E. Vogt, R. C. Malenka, R. A. Nicoll, *Nature* **385**, 630 (1997).
15. M.-Y. Min, D. A. Rusakov, D. M. Kullmann, *Neuron* **21**, 561 (1998).
16. L. A. Schrader, J. G. Tasker, *J. Neurophysiol.* **77**, 527 (1997).
17. G. Tong, C. E. Jahr, *Neuron* **13**, 1195 (1994).
18. J. S. Diamond, C. E. Jahr, *J. Neurosci.* **71**, 4672 (1997).
19. G. Liu, S. Choi, R. W. Tsien, *Neuron* **22**, 395 (1999).
20. A. B. Brussaard *et al.*, *Neuron* **19**, 1103 (1997).
21. D. A. Poulain, J. B. Wakerley, *Neuroscience* **7**, 773 (1982).
22. P. Jourdain *et al.*, *J. Neurosci.* **18**, 6641 (1999).
23. J. S. Isaacson, *Neuron* **23**, 377 (1999).
24. V. Gallo, C. A. Ghiani, *Trends Pharmacol. Sci.* **21**, 252 (2000).
25. P. R. Laming *et al.*, *Neurosci. Biobehav. Rev.* **24**, 295 (2000).
26. L. M. Garcia-Segura, F. Naftolin, J. B. Hutchison, I. Azcoitia, J. A. Chowen, *J. Neurobiol.* **40**, 474 (1999).
27. J. A. Mong, M. M. McCarthy, *J. Neurobiol.* **40**, 602 (1999).
28. S. H. R. Oliet, D. A. Poulain, *J. Physiol.* **520**, 815 (1999).
29. We thank D. T. Theodosis for helpful discussions and comments on the manuscript. Supported in part by grants from the Conseil Régional d'Aquitaine (970301209) and from the Association pour la Recherche Médicale en Aquitaine. R.P. is supported by the French Ministry of Education.

19 January 2001; accepted 8 March 2001

Glia-Synapse Interaction Through Ca^{2+}-Permeable AMPA Receptors in Bergmann Glia

Masae Iino,[1,2] Kaori Goto,[1,2] Wataru Kakegawa,[1,2] Haruo Okado,[2,3] Makoto Sudo,[1] Shogo Ishiuchi,[1,2] Akiko Miwa,[2,3] Yukihiro Takayasu,[1,2] Izumu Saito,[4] Keisuke Tsuzuki,[1,2] Seiji Ozawa[1,2]*

Glial cells express a variety of neurotransmitter receptors. Notably, Bergmann glial cells in the cerebellum have Ca^{2+}-permeable α-amino-3-hydroxy-5-methyl-4-isoxazolepropionic acid (AMPA)–type glutamate receptors (AMPARs) assembled without the GluR2 subunit. To elucidate the role of these Ca^{2+}-permeable AMPARs, we converted them into Ca^{2+}-impermeable receptors by adenoviral-mediated delivery of the GluR2 gene. This conversion retracted the glial processes ensheathing synapses on Purkinje cell dendritic spines and retarded the removal of synaptically released glutamate. Furthermore, it caused multiple innervation of Purkinje cells by the climbing fibers. Thus, the glial Ca^{2+}-permeable AMPARs are indispensable for proper structural and functional relations between Bergmann glia and glutamatergic synapses.

AMPARs are expressed ubiquitously in both neurons and glial cells (*1–3*). Although they are known to mediate fast excitatory synaptic transmission in most brain neurons, their function in glia is uncertain. AMPARs are assembled from the four subunits, GluR1 through GluR4, either alone or in various combinations. The functional properties of AMPARs depend on their subunit composition: AMPARs possessing the GluR2 subunit exhibit either a linear or outwardly rectifying current-voltage (*I-V*) relation and little Ca^{2+} permeability, whereas receptors lacking GluR2 show strong inward rectification and high Ca^{2+} permeability (*4, 5*). In Bergmann glia, only GluR1 and GluR4 mRNAs are expressed; therefore, their AMPARs exhibit inward rectification and are highly permeable to Ca^{2+} (*6–8*).

To elucidate the functional role of the Ca^{2+} permeability of AMPARs in Bergmann glia, we attempted to convert Ca^{2+}-permeable AMPARs into Ca^{2+}-impermeable receptors by adenoviral-mediated delivery of the GluR2 gene. We constructed two recombinant adenoviruses: one for expression of Cre recombinase (AxCANCre) and another bearing a switching unit that consisted of the CAG promoter, a stuffer flanked by a pair of *loxP* sites, and GluR2 cDNA (AxCALNLGluR2) (*9*). We injected these two recombinant adenoviruses together with the recombinant adenovirus bearing green fluorescent protein (GFP) cDNA (AxCAGFP) into the molecular layer of the cerebellar cortex of 20- to 24-day-old rats. Because the adenovirus has much higher affinity to glial cells than neurons, expression of both GFP and GluR2 was detected predominantly in Bergmann glia in the infected areas 2 days after inoculation (Fig. 1, A through C) (*9*). The number of plaque-forming units (PFU) of AxCAGFP in the viral mixture for injection was adjusted to 1/4 to 1/40 the number of PFU of AxCALNL-GluR2 so expression of GluR2 was detected in almost all Bergmann glial cells emitting GFP fluorescence. GFP and GluR2 were detected simultaneously, even when they were expressed in single isolated glia (Fig. 1, D through F). In some experiments, we coexpressed GluR2 and GFP in Bergmann glia using a recombinant adenovirus bearing GluR2 cDNA, the internal ribosomal entry site (IRES) sequence, and GFP cDNA (AxCALALGluR2-IRES-GFP) (*9*). In Bergmann glia infected with this recombinant virus together with AxCAN-Cre, we also detected simultaneous expression of GFP and GluR2.

We next examined the effects of GluR2 expression on the electrophysiological properties of AMPARs in Bergmann glial cells (*9*). We recorded current responses to the iontophoretic application of AMPA in the presence of 50 μM cyclothiazide (CTZ), which reduces desensitization of AMPARs (*10–12*) (Fig. 2). In Bergmann glia without expression of GluR2 in slices infected with AxCALNLGluR2 and AxCAGFP but without AxCANCre, the *I-V* relation invariably exhibited strong inward rectification. The permeability to Ca^{2+} of AMPARs was examined by substituting Na^+-free, 10 mM Ca^{2+} solution for normal saline (*13*). AMPA elicited inward currents at potentials more negative than –20 mV in Na^+-free, 10 mM Ca^{2+} solution ($n = 10$), indicating a high permeability to Ca^{2+} (the ratio of the permeability coefficients of Ca^{2+} and Cs^+, $P_{Ca}/P_{Cs} \approx 2.7$) (Fig. 2A, left). Two days after infection with the three recombinant viruses (AxCALNLGluR2, AxCAGFP, and AxCANCre), the degree of inward rectification was markedly attenuated in Bergmann glia emitting GFP. In 14 of 23 cells (61%), the *I-V* relation of AMPARs exhibited outward rectification, and AMPA elicited no inward current in Na^+-free, 10 mM Ca^{2+} solution at –80 mV, indicating negligible permeability to Ca^{2+} ($P_{Ca}/P_{Cs} < 0.17$) (Fig. 2A, right). To quantify the degree of rectification, we introduced the rectification index (RI), defined as the conductance of the AMPA response measured at +40 mV divided by the conductance at –60 mV (*14*). The RIs were <0.25 in all 21 cells without GluR2 expression (0.13 ± 0.02), and those in 23 cells with GluR2 expression ranged

[1]Gunma University School of Medicine, Maebashi, Gunma 371-8511, Japan. [2]Core Research for Evolutional Science and Technology, Japan Science and Technology Corporation, Kawaguchi, Saitama 332-0012, Japan. [3]Department of Neurobiology, Tokyo Metropolitan Institute for Neuroscience, Fuchu 183-8526, Japan. [4]Institute of Medical Science, University of Tokyo, Tokyo 108-0071, Japan.

*To whom correspondence should be addressed. E-mail: ozawas@med.gunma-u.ac.jp